Corrosion Science 84 (2014) 21–29

Contents lists available at ScienceDirect

Corrosion Science

journal homepage: www.elsevier.com/locate/corsci

A new corrosion inhibitor for copper protection

G. Tansuğ [a,*], T. Tüken [b], E.S. Giray [b], G. Fındıkkıran [b], G. Sığırcık [b], O. Demirkol [b], M. Erbil [b]

[a] Cukurova University, Ceyhan Engineering Faculty, Chemical Engineering, 01960 Adana, Turkey
[b] Cukurova University, Sciences & Letters Faculty, Chemistry Department, 01330 Adana, Turkey

ARTICLE INFO

Article history:
Received 20 August 2013
Accepted 3 March 2014
Available online 12 March 2014

Keywords:
A. Copper
B. EIS
C. Acid corrosion

ABSTRACT

Methyl 3-((2-mercaptophenyl)imino)butanoate (MMPB) was synthesized as inhibitor compound for copper protection. The molecule was designed with azole, thiol functional groups and carboxylate tail group. The inhibition efficiency was examined in acidic chloride media, by means of various electrochemical and spectroscopy techniques. Electrochemical study results showed that high efficiency of MMPB was mainly related with its capability of complex formation with Cu(I) at the surface. The thiol group also improves the adsorptive interaction with the surface, as the carboxylate groups provide extra intermolecular attraction.

1. Introduction

Protection of copper is of particular interest, especially in acidic media which also includes chloride ions [1–16]. Copper is vulnerable against corrosion in such severe environment, although it is highly resistant in nearly neutral or slightly alkaline aqueous environment [2,17–36]. The use of an appropriate inhibitor is necessary, taking into account the specific corrosion mechanism of copper in acidic chloride environment. Especially, in heat exchangers, cooling water system pipelines copper surface is exposed to locally attack of various aggressive species [21]. Local defects and pitting are highly important risks to be handled for copper protection in chloride solution [37–40]. Generally, film assembling inhibitors based on the green chemicals are preferred for this purpose [41–44].

The use of nitrogen and sulfur containing organic compounds as corrosion inhibitor for copper has been widely investigated [1,2,45–51]. Azole compounds tailored with hydrophobic end groups are very popular. The azole group is able to form coordinative covalent bond with vacant d orbitals of copper atoms. Also rings containing conjugated bonds (π electrons) positively affect the interactions between copper and inhibitor compound. There are many reports about various azole group organic inhibitors forming complexes with copper ions and generating highly protective film chemisorbed on the surface. The film built over Cu(I) complex which is inert, insoluble and long lasting polymer like structure [1,2,52].

Also, mercapto group (−SH) containing inhibitors are able to form stable complex with copper ions via the thiolate bond. Most of these inhibitors are modified with an aromatic ring which has certain substituents, in order to increase hydrophobicity on top of protective layer. The inhibition mechanism is based on chemisorption of complex between inhibitor and copper ions, on the surface. The inhibition efficiency is governed by the position of –SH group on the ring (ortho > meta > para) [41,43,53–56].

Methyl 3-((2-mercaptophenyl)imino)butanoate was synthesized as inhibitor compound, the molecule is functionalized with both azole and thiol groups. These groups generate strong adsorptive interaction with metals/alloys, especially in acidic environment. Also, the carboxylate end group has significant dipole character and results with important intermolecular interaction between the molecules adsorbed on the metal surface. Once the adsorbed molecules interact with each other along the carboxylate tails, a film like adsorption layer could be formed on the surface. The inhibition efficiency of this organic compound was investigated against copper corrosion, in 0.1 M HCl solution. The effect of temperature, concentration and extending exposure periods were investigated.

2. Experimental

2.1. Synthesis of inhibitor

Methyl 3-((2-mercaptophenyl)imino)butanoate (MMPB) was synthesized in our laboratory. For synthesis of the inhibitor a mixture of 2-aminobenzenethiol (1.25 g, 10 mmol) and methylacetoacetate (1.26 g, 10 mmol) and %10 mol of trifloroaceticacid (TFA) in 5 ml ethanol in a round bottom flask was stirred at 80 °C

* Corresponding author.
E-mail address: ttuken@cu.edu.tr (G. Tansuğ).

http://dx.doi.org/10.1016/j.corsci.2014.03.004
0010-938X/

in an oil bath. Thin layer chromatography (TLC) of the reaction mixture after 150 min showed the completion of the reaction. Then, the mixture reaction was filtered, and the solid was washed with ethyl acetate. The filtrate was then evaporated under reduced pressure to give the crude product. The pure product was crystallized from ethanol. A general reaction of the synthesized inhibitor was given in Fig. 1.

2.2. Characterization of MMPB

We have synthesized methyl 3-((2-mercaptophenyl)imino)butanoate (MMPB) which is an imine compound [57,58]. The reaction was a facile reaction due to the good electrophilic and nucleophilic properties of β-ketoester compound and amine compound, respectively. The condensation of 2-aminobenzenthiol with methylacetoacetate afforded 85% yield in 150 min at 80 °C, with catalysis of TFA. The yellow colored product was recrystallized from ethanol solution. The characterization of the inhibitor was realized with NMR spectroscopic analysis. The NMR data of inhibitor was given below.

^{1}H NMR (600 MHz, $DMSO_4$-d_6) δ ppm: 6.97 (d, J = 7.8 Hz, 1H), 6.82 (d, J = 7.2 Hz, 1H), 6.57–6.50 (m, 2H), 3.61 (s, 3H), 3.33 (s, 1H), 3.01–2.92 (m, 2H), 1.70 (s, 3H) ^{13}C NMR (150 MHz, $DMSO_4$-d_6) δ ppm: 170.58, 146.57, 125.59, 121.75, 118.99, 109.54, 75.16, 51.93, 48.06, 29.57.

The stability of MMBP against hydrolysis was examined in acidic corrosive environment. The synthesized molecule is an imine compound and these species may undergo hydrolysis in order to yield amine and carbonyl compounds, in highly acidic media. For this purpose, 10 mM inhibitor containing test solution (0.10 M HCl) was stirred continuously for an hour, under 45 °C temperature. Then, samples were taken from this solution and analyzed with help of FTIR (Fourier transformed infrared). The solution was mixed KBr and pellets were prepared. The obtained spectra revealed that there was not any amine group, since there was not any absorption peak between 3443 and 3357 cm^{-1}. Also, there was no evidence for any other possible hydrolysis product.

2.3. Electrochemical studies

Electrochemical studies were realized in 0.1 M HCl test solution, employing three electrodes setup in one compartment cell. A platinum sheet was utilized as the counter electrode and Ag/AgCl (3 M KCl) was the reference. The working electrode was copper (99.99% purity) cylindrical rod embedded in resin, with one bottom surface (0.283 cm^2) open to exposure. Before each experiment, the specimens were mechanically abraded with silicon carbide papers (from grades 500 to 1000), degreased with acetone, washed with distilled water and dried.

For studies aiming to determine corrosion rate with quantitative analysis of immersion test solutions, square shaped (10 × 10 × 1 mm) copper (99.99% purity) coupons were utilized. The surface of these samples was prepared with the same route as described above.

CHI 660C model electrochemical workstation was employed for potentiodynamic, ac impedance measurements. Before each electrochemical test, the potential of the electrode was monitored

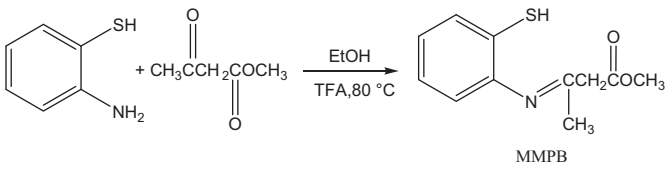

Fig. 1. The synthesis reaction of inhibitor compound.

with time until the steady state conditions set on the electrode surface. Then, the measured stable electrode potential was handled as the corrosion potential (E_{corr}). It was seen that approximately 30 min was sufficient for reaching the said steady state, in presence and absence of inhibitor in test solution. Potentiodynamic method was used to obtain anodic polarization plots, starting from E_{corr} value and employing 1 mV/s scan rate. EIS measurements were realized at E_{corr} value, with 5 mV perturbation voltage in a frequency range of 10^{+4}–10^{-2} Hz.

In order to clarify the inhibition mechanism, the effect of concentration and temperature were studied separately. The temperature range was between 25 and 55 °C, which was valid for many open cooling water systems. The concentration range was selected in between 0.5 and 10 mM inhibitor, for the purpose of less chemical consumption in practical applications.

In order to investigate the morphology and structural composition of the surface, Zeiss/Supra 55 model FE-SEM (field emission scanning electron microscope) equipped with EDX was utilized. Copper coupons were immersed in blank and 10 mM inhibitor containing solutions, for 7 days.

3. Results and discussion

3.1. Corrosion inhibition studies

Before realization of potentiodynamic and electrochemical measurements, steady state conditions must be provided on the electrode surface. In Fig. 2, the corrosion potential (E_{corr}) of copper electrodes are plotted against immersion time. It is clear that stable corrosion potential value is reached in about 30 min, for both inhibitor free and 10 mM inhibitor containing solutions. Then before each electrochemical measurement, 30 min immersion time was employed for each electrode.

In Fig. 3, potentiodynamic measurement results are given for copper in the absence and presence of 10 mM MMPB, in 0.1 M HCl. In inhibitor free solution, copper dissolution leads to formation of sparingly soluble copper (I) chloride (K_{sp}: 1.72×10^{-7}) on the surface [41,59]. None of the copper oxides are stable under studied pH conditions and anodic dissolution rate is directly related to barrier effect of CuCl deposit on the surface. This event is observed as a wide peak in the potential range of −0.02 and +0.08 V (vs. Ag/AgCl). Once the surface is covered with CuCl, this deposit exhibits a physical barrier between the solution and metal. Then the anodic dissolution rate (thus the current density) was controlled by the stability of this CuCl layer and limitation of mass transfer. The anodic dissolution of copper has been extensively discussed in the literature, considering various mechanism steps in order to explain the kinetics of dissolution properly [10,24]. In our case, the following steps are considered to explain the potentiodynamic measurement results. The first irreversible reaction (Eq. (1)) defined the general pattern observed at earlier potential region of anodic plots, at which the film formation is completed and a maximum peak current density is observed. Then the charge transfer becomes controlled with the mass transfer limitation of protective layer. The Eqs. (2) and (3) explain the current density increase due to formation of Cu(II) species, under high potentials.

$$Cu + Cl^- \rightarrow CuCl_{(ads)} + e \quad (1)$$

$$CuCl_{(ads)} + Cl^- \leftrightarrow CuCl^-_{2(ads)} \quad (2)$$

$$CuCl^-_{2(ads)} \leftrightarrow Cu^{2+} + 2Cl^- + e \quad (3)$$

In the case of 10 mM MMPB containing solution, the current density value was quite lower than inhibitor free conditions. Also, the peak attributed to Cu(I) chloride formation disappeared. This

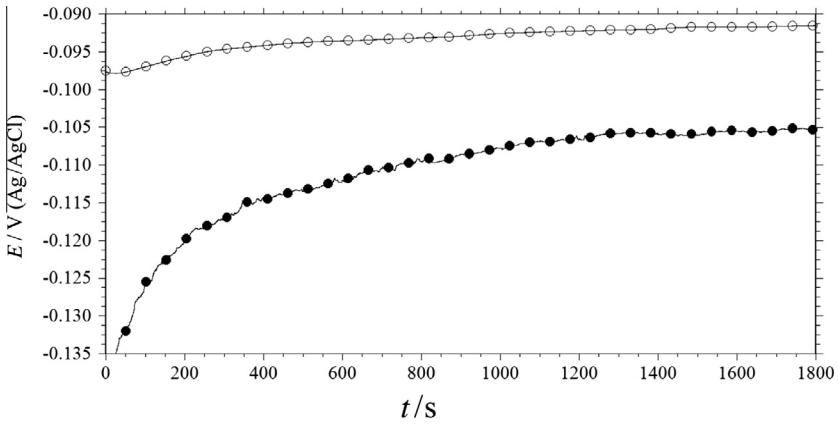

Fig. 2. Open circuit potential (E_{ocp})-time plots for copper electrodes in inhibitor free (○) and +10 mM MMBP (●) solutions.

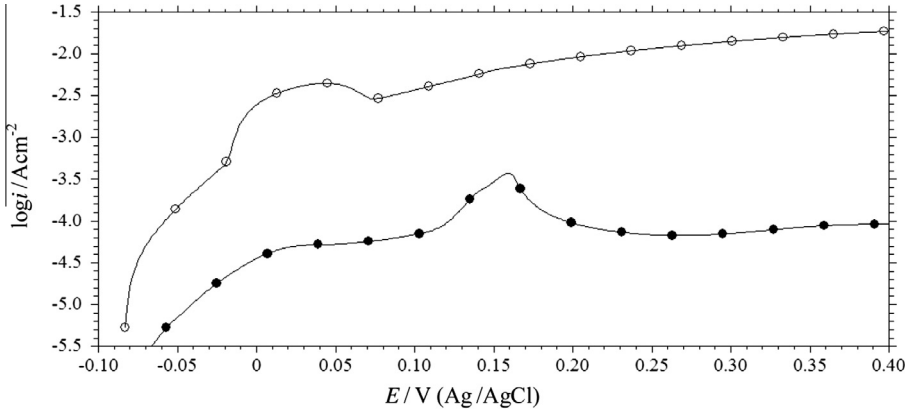

Fig. 3. Anodic polarization plots for copper after 30 min exposure time in 0.1 M HCl solutions, inhibitor free (○) and +10 mM MMPB (●) solutions.

case could only be explained with strong interaction between the MMPB molecules and the surface. During the period prior to measurement, the surface has already been covered with Cu(I) chloride deposit and inhibitor adsorption layer [41]. The peak appeared between 0.10 and 0.20 V (vs. Ag/AgCl) was attributed to completion of protective film layer with help of Cu(I)–MMPB complex formation on the surface. It is well known that cupric and cuprous ions are able to form stable complexes with organic inhibitors tailored with azole functional groups. According to dissolution mechanism of copper, Cu(I) is formed at the first step. Then, these ions could form protective complex with inhibitor or chloride ions at the interface, soon. Then the current density value remained almost constant in a wide potential range. This means that the anodic dissolution rate is under diffusion control.

In order to evaluate the effect of chloride ions on inhibition mechanism, potentiodynamic measurements were repeated in chloride free solution (0.05 M H_2SO_4) provided that the hydronium ion concentration was the same, Fig. 4. In order to understand the complex formation and efficiency of MMPB, the anodic polarization plots are given for 0.05 M H_2SO_4 solution, Fig. 4. In inhibitor free solution, dissolution of copper was mainly activation controlled at potentials close to E_{corr} value. Under studied pH, neither Cu(I) nor Cu(II) oxide are stable and anodic dissolution occurs readily as the potential increases. At higher potentials, the current density is governed by diffusion limitations through the solution [8,9,60].

In the case of inhibitor added solution, the anodic dissolution is controlled by the mass transport limitation, near the corrosion potential. As soon as Cu(I) intermediate appeared at the interface, these ions interact with the adsorbed inhibitor molecules and the surface is covered with protective layer. During the scan, the current density value could be considered as limiting current at potentials close to E_{corr}. At higher potentials, the oxidation of Cu(I) to Cu(II) takes place and higher anodic current densities are observed.

$$Cu \leftrightarrow Cu(I)_{ads} + e \quad (4)$$

$$Cu + Cu(I)_{ads} \rightarrow Cu(II)_{sol} + Cu(I)_{ads} + 2e \quad (5)$$

$$Cu(I)_{ads} \leftrightarrow Cu(II)_{ads} + e \quad (6)$$

$$Cu + Cu(II)_{ads} \rightarrow Cu(II)_{sol} + Cu(II)_{ads} + 2e \quad (7)$$

EIS measurements were also realized for evaluation of inhibition efficiency of MMPB. The results obtained for inhibitor free conditions are given in Fig. 5. The circuit model used for fitting is given in Fig. 6 [61]. The EIS results clearly indicated to diffusion controlled charge transfer process and this was corroborating with the discussions up to now, about the effect of CuCl deposit on the surface [41]. The deposit of copper (I) chloride creates some kind of barrier effect on the surface. The corrosion process could take place at the regions where the surface is uncovered. In fact, the rate of $[CuCl_2^-]$ formation is crucial (Eq. (2)) for corrosion rate; this non electrochemical step controls the whole corrosion process.

In Fig. 7, it is seen that inhibitor addition caused to formation of highly stable protective layer on the surface. The high barrier efficiency of this layer was mainly related with the formation of Cu(I)–inh complex, as discussed before. However, the corrosion process cannot be stopped completely. Then, the diffusion of corrosive species must happen along this coating. The Warburg impedance is frequency dependent and since the said film gave

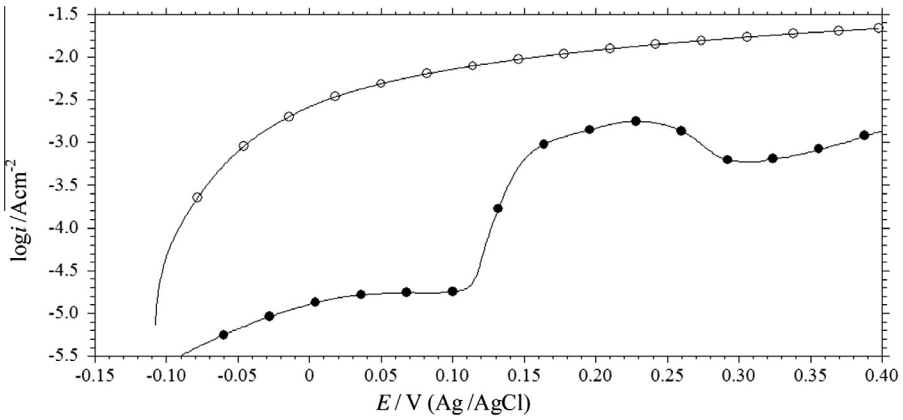

Fig. 4. Anodic polarization plots for copper after 30 min exposure time in 0.05 M H_2SO_4 solutions, inhibitor free (○) and +10 mM MMPB (●) solutions.

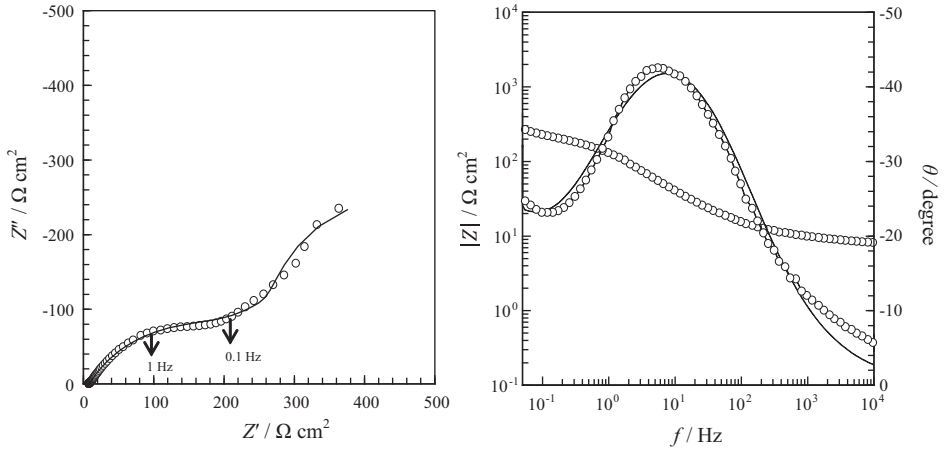

Fig. 5. The fitted EIS results for copper after 30 min exposure time in 0.1 M HCl inhibitor free (○) solutions. The fitting curves are given with solid lines.

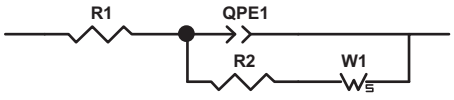

Fig. 6. The equivalent circuit used for fitting the EIS data of inhibitor free solution.

extremely high resistance the effect of diffusion limitation may not be dominant in collected data. Therefore a Warburg element was not utilized for 10 mM inhibitor concentration results; the equivalent circuit was consisted of two time constants and solution resistance. However, it becomes necessary when the inhibitor concentration is very low, because CuCl becomes dominant at the surface.

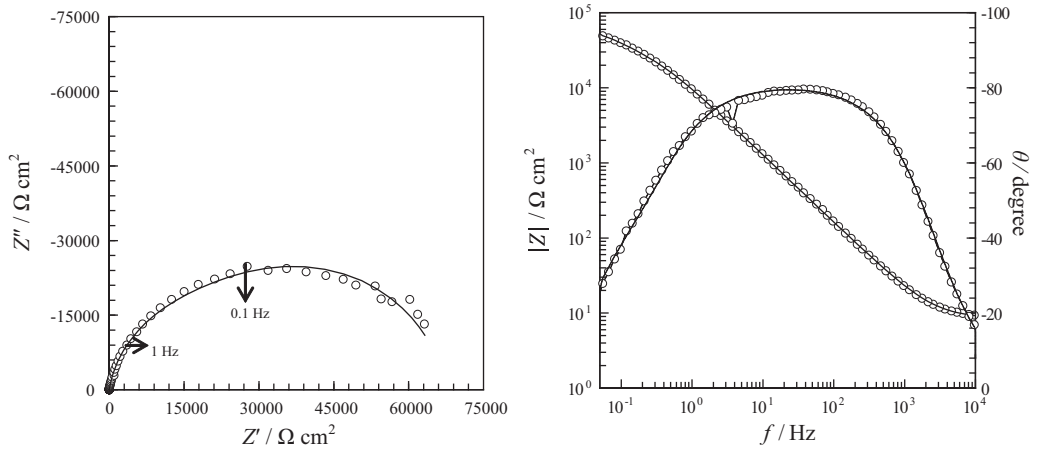

Fig. 7. The fitted EIS results for copper after 30 min exposure time in 0.1 M HCl +10 mM MMPB (○) solutions. The fitting curves are given with solid lines.

According the fitting results, the metal solution interface capacitance ($C_{M/S}$) value decreased from 22.97 to 4.91 μF cm^{-2}. This situation shows that the barrier efficiency was quite well and the corroding surface area is smaller with respect to inhibitor free conditions. This was an evidence for presence of a compact assembled film on the surface. For the same reason, the polarization resistance (R_p) value increased from 430 to 64,500 Ω cm^2. These results are compatible with the potentiodynamic measurement results.

The potentiodynamic polarization results of copper in 0.1 M HCl at 25 °C in presence of MMPB in various concentrations are seen in Fig. 8. The current density values decreased with increasing inhibitor concentration. This was associated with shift of corrosion potential to more positive values. This outcome is related to enrichment of Cu–inh complex deposit on the surface, rather than CuCl. It must be noticed that CuCl formation peak (in the potential range of −0.02 and +0.08 V (vs. Ag/AgCl)) cannot be seen for 5 and 10 mM inhibitor concentrations. At lower inhibitor concentrations (0.5 and 1 mM), this peak is observed. As the inhibitor concentration decreases, the role of less protective CuCl deposit becomes dominant on the surface. For the concentration of 0.5 mM, the current density increased regularly at potentials higher than 0.10 V (vs. Ag/AgCl). Under these circumstances, the surface is mainly covered with CuCl and the inhibitor concentration is quite low around surface. Physical adsorption of inhibitor molecules becomes harder because of inadequate (with respect to high chloride concentration) surface concentration and the anodic current density value increases. There is competitive adsorption on the surface between Cl^- and inhibitor molecules. Once the bulk inhibitor concentration is high enough (5, 10 mM), these molecules can replace the chloride ions from the interface. The strongly adhered inhibitor molecules hinder the formation of CuCl on the surface. At this point of consideration, the functional group (–SH) also plays significant role for adsorption to the copper surface [20,43]. Then the azole group interacts with freshly delivered Cu(I) ions at the interface and the protective complex is formed.

In Fig. 9, the experimental and fitting results are given for different inhibitor concentrations in 0.1 M HCl. The data obtained with fitting of EIS results are summarized in Table 1. The R_p value increased significantly with the concentration and 64,500 Ω cm^2 was obtained with 10 mM inhibitor concentration. This increase was simply explained with highly efficient barrier film on the surface. This R_p value could be utilized for calculation of percent inhibition efficiency (φ) with the following equation.

$$\varphi = \left(\frac{R'_p - R_p}{R'_p}\right) \times 100 \quad (8)$$

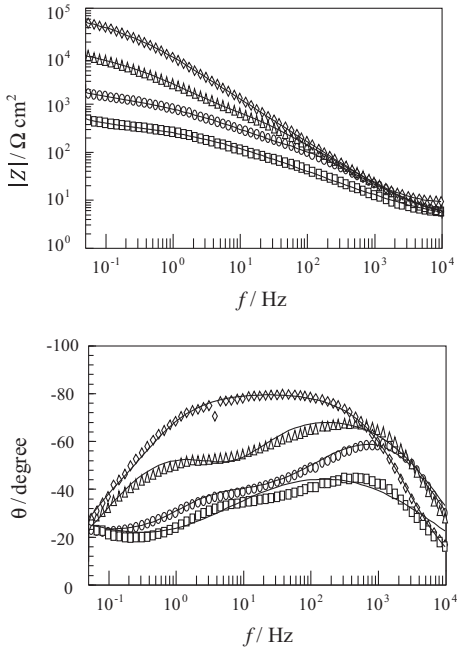

Fig. 9. The fitted EIS results for copper after 30 min exposure time in 0.1 M HCl solution containing 0.5 mM (□), 1 mM (○), 5 mM (Δ) and 10 mM (◇) MMPB. The fitting curves are given with solid lines.

Table 1
The corrosion potential (E_{corr}) polarization resistance (R_p), metal/solution interface capacitance ($C_{M/S}$), inhibition efficiency (φ) for copper in 0.1 M HCl solution containing different concentrations of MMPB.

C (mM)	$C_{M/S}$ (μF) cm^{-2}	E_{corr} (V) (Ag/AgCl)	R_p (Ω cm^2)	φ
0.0	22.97	−0.087	430	–
0.5	13.07	−0.119	860	49.7
1.0	7.77	−0.140	2560	83.1
5.0	5.23	−0.287	13,200	96.7
10.0	4.91	−0.259	64,500	99.3

In this equation R_p and R'_p represent the values measured in the blank and inhibitor added solution. In inhibitor free solutions, only CuCl could be formed on the surface. However this deposit has a physical barrier effect, too. Therefore, the calculated φ values reveal the effect of inhibitor film with respect to CuCl deposit. The percent inhibition efficiency increased regularly with the concentration and 99% value was reached with 10 mM MMPB.

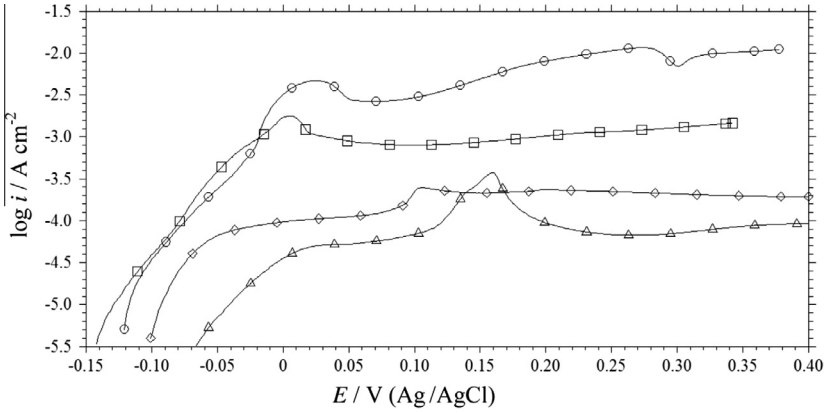

Fig. 8. Anodic polarization plots for copper after 30 min exposure time in 0.1 M HCl solutions containing 0.5 mM (o), 1 mM (□), 5 mM (◇) and 10 mM (Δ) MMPB.

The value of $C_{M/S}$ decreased regularly with the increasing inhibitor concentration, Table 1. As the inhibitor concentration increases, the physical barrier property of protective layer becomes more efficient. However, there are always some pores through the film and corrosive solution finds a path to reach the underlying copper substrate. Each pore could be considered like an electrochemical microcell, at which corrosion takes place. When the permeability of barrier film increases, the number of these microcells and total active metal/solution interface area increase. The decrease of $C_{M/S}$ value has the meaning of higher surface coverage ratio and vice versa. In this study, an accurate value cannot be calculated for surface coverage ratio, with a simple comparison between $C_{M/S}$ values obtained in inhibitor containing and blank solutions [62]. Because the blank solution contains chloride ions and CuCl deposition is inevitable. Then the $C_{M/S}$ value cannot be obtained for totally bare copper surface, in chloride solutions.

3.2. Effect of temperature

In order to test the stability of protective film, the electrochemical experiments were realized under different temperature conditions. The potentiodynamic measurement results are in Fig. 10. In inhibitor free solution, with the temperature the current values increased slightly, due to higher anodic dissolution rate. The solubility of CuCl increases with temperature and the surface becomes more vulnerable against corrosive attack.

The protection efficiency of inhibitor decreased gradually, with the temperature (Fig. 10b). Also, Cu–inh complex formation peak (0.10–0.20 V (vs. Ag/AgCl)) shows tendency to get smaller under elevated temperature conditions. The surface was covered with adsorbed species (inhibitor, CuCl and Cu–inh) but the mass transport kinetics are influenced by temperature increase. The inhibitor still exhibits reasonable efficiency under 55 °C, during the anodic polarization. The azole group played the major role for adsorption, while the carboxylate groups (at the solution side of molecule) interact with other molecules and help the barrier property. The intermolecular attractions between inhibitor molecules weaken at high temperatures.

The EIS results obtained under different temperatures are given in Figs. 11 and 12. From fitting the EIS data some quantities are determined and summarized in Table 2.

It is clear from Table 2, the inhibition efficiency decreased with the temperature. The calculated φ values stated that inhibitor could still decrease the corrosion rate significantly under elevated temperatures, with respect to uninhibited conditions. The capacitance values changed irregularly with temperature. This was related to acceleration of thermal motions of adsorbing species at the interface.

3.3. Effect of exposure time

The inhibition efficiency was also examined with extending exposure period. Identical copper coupons were immersed in inhibitor free and 10 mM inhibitor containing test solutions, for 7 days. The corresponding EDX profile analysis shows that copper (I) chloride is the unique stable compound on the surface, Fig. 13a. In the solution containing 10 mM inhibitor, the chloride peak decreased dramatically, Fig. 13b. This proves that CuCl cannot be found on the surface, when the inhibitor molecules are strongly adsorbed on copper. There is also a sulfur peak next to chloride. Even though its intensity is very low, it is an evidence for the role of sulfur atoms for binding to copper surface. These EDX results prove that the protective film composed of strongly adhered inhibitor molecules, Cu–inh complex and CuCl deposit.

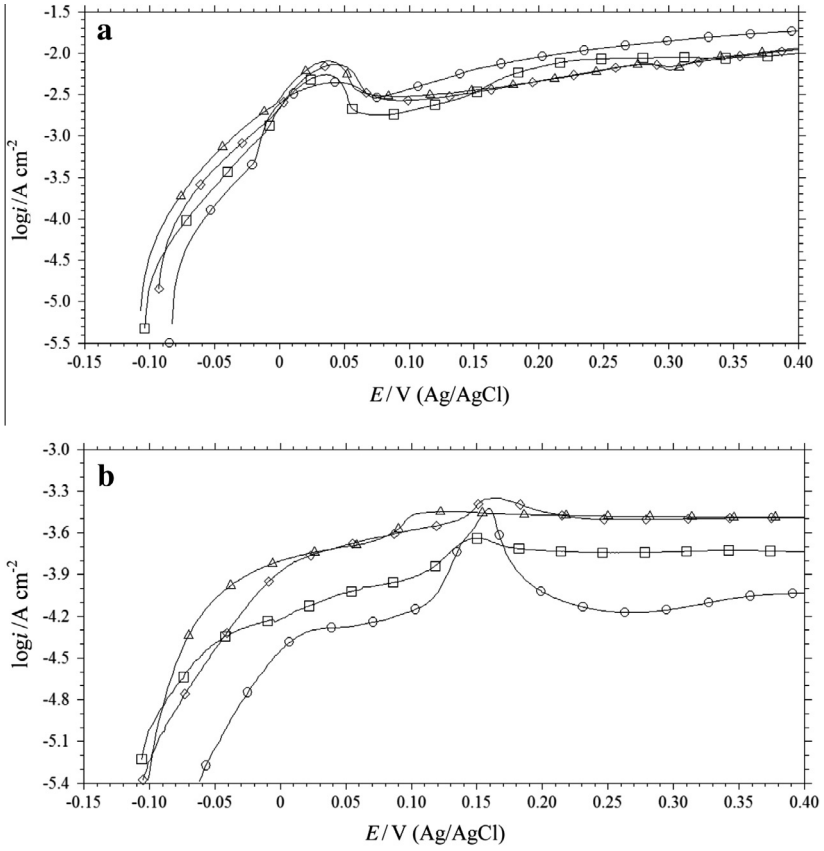

Fig. 10. Anodic polarization plots for copper after 30 min in 0.1 M HCl inhibitor free (a) and +10 mM MMPB (b) solutions; 25 °C (o), 35 °C (□), 45 °C (◇) and 55 °C (Δ).

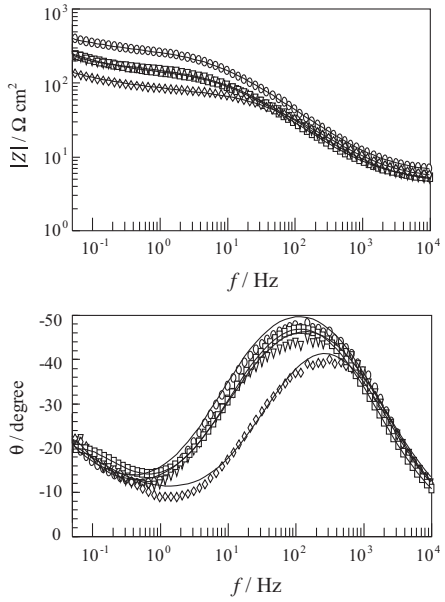

Fig. 11. The fitted Bode plots for copper after 30 min exposure time in 0.1 M HCl inhibitor free solution; 25 °C (○), 35 °C (□), 45 °C (▽) and 55 °C (◇). The fitting curves are given with solid lines.

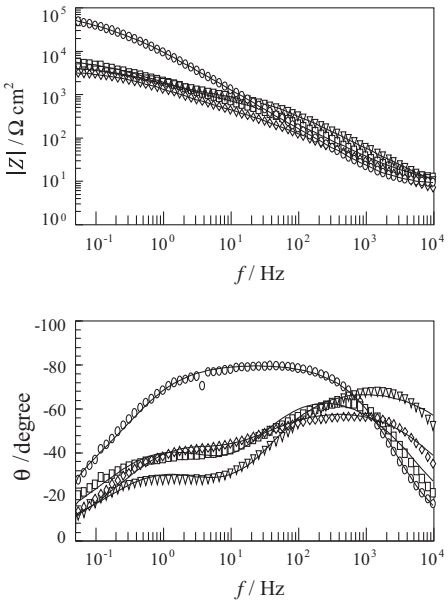

Fig. 12. The fitted Bode plots for copper after 30 min exposure time in 0.1 M HCl solution 10 mM MMPB; 25 °C (○), 35 °C (□), 45 °C (▽) and 55 °C (◇). The fitting curves are given with solid lines.

Table 2
The capacitance values of copper in absence ($C^{o}_{M/S}$) and 10 mM inhibitor containing ($C_{M/S}$) solutions and inhibition efficiency (φ) values calculated under different temperatures.

T (°C)	$C^{o}_{M/S}$ (μF cm^{-2})	$C_{M/S}$ (μF cm^{-2})	R^{o}_{p} (Ω cm^2)	R_p (Ω cm^2)	φ
25	22.97	4.91	430	64,500	99.3
35	5.12	4.66	280	16,500	98.3
45	6.40	1.38	255	4440	94.3
55	6.75	1.79	250	3450	92.7

SEM measurements were realized for these samples exposed to 7 days immersion test. The surface was highly deteriorated, under inhibitor free conditions (Fig. 14a). Copper (I) chloride deposition may have covered the surface, but this compound is subjected to further oxidation to Cu(II) species and dissolution, as discussed in earlier sections (Eqs. (2) and (3)). Thus the surface was still vulnerable against attack of corrosive species. Moreover, it is apparent that some regions are abraded at a higher ratio, due to some microstructural differences from side to side. The surface was highly rough, at the end of immersion test in blank solution. In Fig. 14b, it was clearly seen that the MMPB hindered the attack of corrosive species, successfully. The smooth surface was indicative for significant physical barrier behavior of adsorbed inhibitor molecules between the metal and corrosive environment. According to given EDX analysis results (Fig. 13), Cu(I) chloride deposit is formed at the regions which are not covered with inhibitor.

The inhibition efficiency against copper corrosion was also examined for extending immersion periods. For this purpose, copper electrodes were immersed in blank and +10 mM MMPB test solutions. The MMPB was shown to have significant efficiency even after prolonged exposure time; the R_p value was 8500 Ω cm^2, where the R_p value was 184 Ω cm^2 (Fig. 15). From fitting results, the efficiency seems to be very high. Also, the capacitive behavior of the interface occupied extremely wide frequency range that the beginning of this region falls out of the range. This shows that the protective layer is highly stable and hinders the charge transfer between metal and corrosive solution.

After 7 days exposure tests, the solutions were analyzed with AAS for quantitative measurement of copper ions released due to corrosion. During this immersion period, the inhibitor added solution remained colorless as the inhibitor free solution turned into bluish green color due to intense copper corrosion. These solutions were analyzed with AAS and dissolved copper amounts were determined to be 592.518 and 20.126 mg L^{-1}, for inhibitor free and inhibitor containing solutions respectively. These values could be utilized to obtain corrosion rate. Applying the Faraday's Laws, corrosion current (i_{corr}) values [63] were calculated as 7.45×10^{-5} and 2.53×10^{-6} A cm^{-2}, for inhibitor free and 10 mM inhibitor containing conditions respectively. According to test results of 7 days immersion period, the protection efficiency is found to be 96.60%. This efficiency value is in accord with the efficiency results given from evaluation of electrochemical measurement results. However, it is slightly lower than the efficiency obtained from comparison of R_p values. There is a risk of under/over estimation with the use of R_p value for evaluation of corrosion rate/protection efficiency. Since the measured resistance value includes all the resistive contributions, even they are caused by non-protective and weakly adsorbed species along the distance from metal surface through the solution. Frequently, the i_{corr} value is tried to be obtained from evaluation of Tafel regions of potentiodynamic measurement results. However, in such environment that the copper surface is covered with Cu(I) compounds soon, it is very difficult to obtain and evaluate the Tafel regions accurately. Since the overall metal dissolution process is controlled by mass transport limitation. Therefore the solution assay analysis results are considered to give more accurate results for corrosion rate. In the literature, 90.80% inhibition efficiency was reported for 10 mM benzotriazole (BTA) in 0.1 M HCl acid solution [1]. Higher efficiency values were reported when a thiol group is also attached to inhibitor molecule, for example 4-amino-4H-1,2,4-triazole-3-thiol exhibits 91.38%, in acidic chloride solution [3]. In another study, the efficiency of 5-methyl benzotriazole was reported to be 97.87% [1]. The inhibition efficiency of MMBP is quite well, when compared to others reported in the literature. Also, it was shown that the efficiency of MMBP is not lost with extending exposure periods.

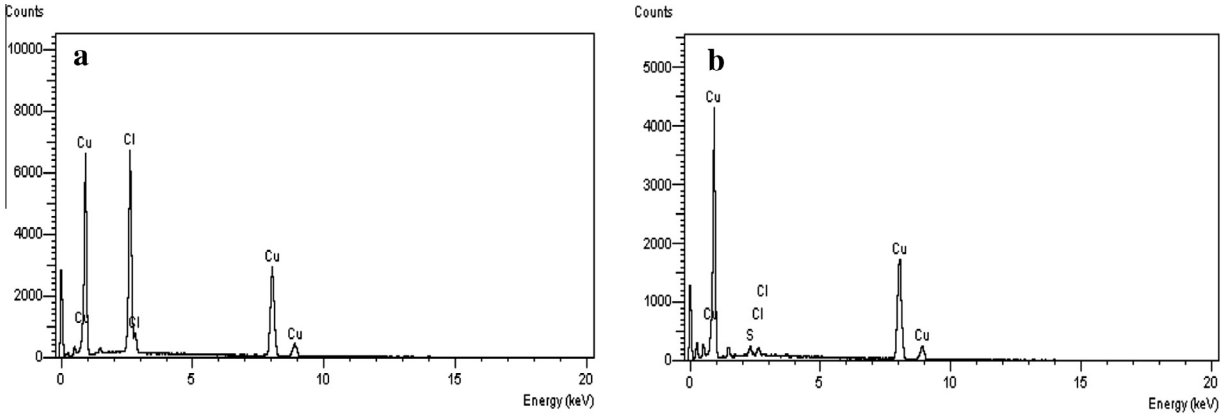

Fig. 13. EDX analysis results of copper surface after 7 days immersion time in 0.1 M HCl (a) and 0.1 M HCl +10 mM inhibitor (b) solutions at 25 °C.

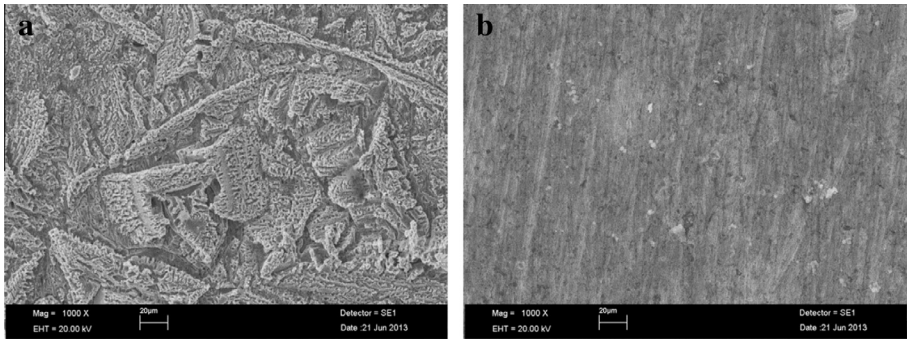

Fig. 14. SEM images of copper coupons after 7 days exposure to 0.1 M HCl (a) and 0.1 M HCl +10 mM inhibitor (b).

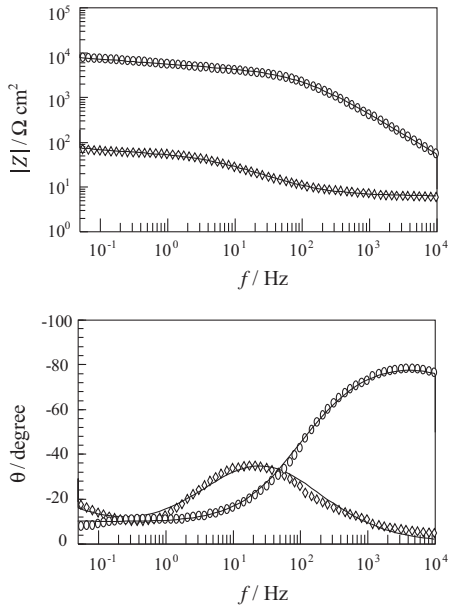

Fig. 15. The fitted EIS results after 7 days immersion period in inhibitor free (◇) and +10 mM inhibitor (○) solution. The fitted results are shown with solid line.

4. Conclusions

The synthesized compound methyl 3-((2-mercaptophenyl)imino)butanoate was exhibited very high inhibition efficiency against copper corrosion in acidic chloride environment. The inhibition mechanism was explained with complex formation between the inhibitor and Cu(I) ions at the interface. Also the thiol group of the molecule improves the adsorptive interaction with the copper surface. The protection efficiency increased with increasing inhibitor concentration, and 99.30% efficiency of 10 mM concentration. The durability of protective film was found to be good against temperature increase; the efficiency was 92.70% at 55 °C. The protection efficiency was also good for extending periods, 96.60% efficiency was determined, after 7 days exposure to 10 mM inhibitor containing test solution. Also, the SEM results proved that the inhibitor could successfully protect the copper surface for considerably 7 days exposure period.

References

[1] M.M. Antonijevic, B.M.B. Petrovic, Copper corrosion inhibitors, A Rev. Int. J. Electrochem. Sci. 3 (2008) 1–28.
[2] M.M. Antonijevic, S.M. Milic, M.B. Petrovic, Films formed on copper surface in chloride media in presence of azoles, Corros. Sci. 51 (2009) 1228–1237.
[3] Sudheer, M.A. Quraishi, Electrochemical and theoretical investigation of triazole derivatives on corrosion inhibition behavior of copper in hydrochloric acid medium, Corros. Sci. 70 (2013) 161–169.
[4] M. Scendo, Potassium ethyl xanthate as corrosion inhibitor for copper in acidic chloride solutions, Corros. Sci. 47 (2005) 1738–1749.
[5] E. Szőcs, Gy. Vastag, A. Shaban, E. Kálmán, Electrochemical behaviour of an inhibitor film formed on copper surface, Corros. Sci. 47 (2005) 893–908.
[6] El-Sayed M. Sherif, R.M. Erasmus, J.D. Comins, Effects of 3-amino-1,2,4-triazole on the inhibition of copper corrosion in acidic chloride solutions, J. Colloid Interf. Sci. 311 (2007) 144–151.
[7] J.B. Matos, L.P. Pereira, S.M.L. Agostinho, O.E. Barcia, G.G.O. Cordeiro, E. D'Elia, Effect of cysteine on the anodic dissolution of copper in sulfuric acid medium, J. Electroanal. Chem. 570 (2004) 91–94.
[8] G.G.O. Cordeiro, O.E. Barcia, O.R. Mattos, Copper electro dissolution mechanism in a 1M sulphate medium, Electrochim. Acta 38 (1993) 319–324.
[9] J.B. Matos, E. D'Elia, O.E. Barcia, O.R. Mattos, N. Pébère, B. Tribollet, Rotating disc and hemispherical electrodes for copper dissolution study in hydrochloric solution in the presence of benzotriazole, Electrochim. Acta 46 (2001) 1377–1383.

[10] H.O. Curkovic, E. Stupnisek-Lisac, H. Takenouti, The influence of pH value on the efficiency of imidazole based corrosion inhibitor of copper, Corros. Sci. 52 (2010) 398–405.
[11] H. Ma, S. Chen, B. Yin, S. Zhao, X. Liu, Impedance spectroscopic study of corrosion inhibition of copper by surfactants in the acidic solutions, Corros. Sci. 45 (2003) 867–882.
[12] G. Quartarone, M. Battilana, L. Bonaldo, T. Tortato, Investigation of the inhibition effect of indole-3-carboxylic acid on the copper corrosion in 0.5 M H_2SO_4, Corros. Sci. 50 (2008) 3467–3474.
[13] K.F. Khaled, Mohammed A. Amin, Dry and wet lab studies for some benzotriazole derivatives as possible corrosion inhibitors for copper in 1.0 M HNO3, Corros. Sci. 51 (2009) 2098–2106.
[14] N. Huynh, S.E. Bottle, T. Notoya, A. Trueman, B. Hinton, D.P. Schweinsberg, Studies on alkyl esters of carboxybenzotriazole as inhibitors for copper corrosion, Corros. Sci. 44 (2002) 1257–1276.
[15] M.M. El-Naggar, Bis-aminoazoles corrosion inhibitor for copper in 4.0 M HNO_3 solutions, Corros. Sci. 42 (2000) 773–784.
[16] D.Q. Zhang, Q.R. Cai, X.M. He, L.X. Gao, G.S. Kim, The corrosion inhibition of copper in hydrochloric acid solutions by a tripeptide compound, Corros. Sci. 51 (2009) 2349–2354.
[17] F. Zucchi, G. Trabanelli, M. Fonsati, Tetrazole derivatives as corrosion inhibitors for copper in chloride solutions, Corros. Sci. 38 (1996) 2019–2029.
[18] M. Finšgar, EQCM and XPS analysis of 1,2,4-triazole and 3-amino-1,2,4-triazole as copper corrosion inhibitors in chloride solution, Corros. Sci. 77 (2013) 350–359.
[19] H.O. Curkovic, E. Stupnisek-Lisac, H. Takenouti, Electrochemical quartz crystal microbalance and electrochemical impedance spectroscopy study of copper corrosion inhibition by imidazoles, Corros. Sci. 51 (2009) 2342–2348.
[20] R. Vera, F. Bastidas, M. Villarroel, A. Oliva, A. Molinari, D. Ramírez, R. del Río, Corrosion inhibition of copper in chloride media by 1,5-bis(4-dithiocarboxylate-1-dodecyl-5-hydroxy-3-methylpyrazolyl)pentane, Corros. Sci. 50 (2008) 729–736.
[21] F. Zucchi, G. Trabanelli, C. Monticelli, The inhibition of copper corrosion in 0.1 M NaCl under heat exchange conditions, Corros. Sci. 38 (1996) 147–154.
[22] K.F. Khaled, Studies of the corrosion inhibition of copper in sodium chloride solutions using chemical and electrochemical measurements, Mater. Chem. Phys. 125 (2011) 427–433.
[23] D. Gopi, K.M. Govindaraju, V.C.A. Prakash, D.M.A. Sakila, L. Kavitha, A study on new benzotriazole derivatives as inhibitor on copper corrosion in ground water, Corros. Sci. 51 (2009) 2259–2265.
[24] G. Kear, B.D. Barker, F.C. Walsh, Electrochemical corrosion of unalloyed copper in chloride media – a critical review, Corros. Sci. 46 (2004) 109–135.
[25] M. Scendo, Inhibition of copper corrosion in sodium nitrate solutions with nontoxic inhibitors, Corros. Sci 50 (2008) 1584–1592.
[26] F. Rosalbino, R. Carlini, F. Soggia, G. Zanicchi, G. Scavino, Influence of rare earth metals addition on the corrosion behaviour of copper in alkaline environment, Corros. Sci. 58 (2012) 139–144.
[27] M.B. Valcarce, M. Vázquez, Phosphate ions used as green inhibitor against copper corrosion in tap water, Corros. Sci. 52 (2010) 1413–1420.
[28] H. Tian, W. Li, B. Hou, Novel application of a hormone biosynthetic inhibitor for the corrosion resistance enhancement of copper in synthetic seawater, Corros. Sci. 53 (2011) 3435–3445.
[29] A. Drach, I. Tsukrov, J. DeCew, J. Aufrecht, A. Grohbauer, U. Hofmann, Field studies of corrosion behaviour of copper alloys in natural seawater, Corros. Sci. 76 (2013) 453–464.
[30] W. Li, L. Hu, S. Zhang, B. Hou, Effects of two fungicides on the corrosion resistance of copper in 3.5% NaCl solution under various conditions, Corros. Sci. 53 (2011) 735–745.
[31] H. Tian, W. Li, K. Cao, B. Hou, Potent inhibition of copper corrosion in neutral chloride media by novel non-toxic thiadiazole derivatives, Corros. Sci. 73 (2013) 281–291.
[32] R. Subramanian, V. Lakshminarayanan, Effect of adsorption of some azoles on copper passivation in alkaline medium, Corros. Sci. 44 (2002) 535–554.
[33] B. Trachli, M. Keddam, H. Takenouti, A. Srhiri, Protective effect of electropolymerized 3-amino-1,2,4-triazole towards corrosion of copper in 0.5 M NaCl, Corros. Sci. 44 (2002) 997–1008.
[34] N. Huynh, S.E. Bottle, T. Notoya, D.P. Schweinsberg, Inhibitive action of the octyl esters of 4- and 5-carboxybenzotriazole for copper corrosion in sulphate solutions, Corros. Sci. 42 (2000) 259–274.
[35] M. Scendo, Inhibitive action of the purine and adenine for copper corrosion in sulphate solutions, Corros. Sci. 49 (2007) 2985–3000.
[36] S.M. Milić, M.M. Antonijević, Some aspects of copper corrosion in presence of benzotriazole and chloride ions, Corros. Sci. 51 (2009) 28–34.
[37] K.M. Ismail, Evaluation of cysteine as environmentally friendly corrosion inhibitor for copper in neutral and acidic chloride solutions, Electrochim. Acta 52 (2007) 7811–7819.
[38] A. El Warraky, H.A. El Shayeb, E.S.M. Sherif, Pitting corrosion of copper in chloride solutions, Anti-Corros. Method M 51 (2004) 52–61.
[39] S.H. Lee, J.G. Kim, J.Y. Koo, Investigation of pitting corrosion of a copper tube in a heating system, Eng. Fail. Anal. 17 (2010) 1424–1435.
[40] A.M. Abdullah, F.M. Al-Kharafi, B.G. Ateya, Intergranular corrosion of copper in the presence of benzotriazole, Scripta Mater. 54 (2006) 1673–1677.
[41] T. Tuken, N. Kicir, N.T. Elalan, G. Sigircik, M. Erbil, Self-assembled film based on hexane-1,6-diamine and 2-mercapto-ethanol on copper, Appl. Surf. Sci. 258 (2012) 6793–6799.
[42] B.V.A. Rao, M.Y. Iqbal, B. Sreedhar, Self-assembled monolayer of 2-(octadecylthio)benzothiazole for corrosion protection of copper, Corros. Sci. 51 (2009) 1441–1452.
[43] Y.S. Tan, M.P. Srinivasan, S.O. Pehkonen, Simon Y.M. Chooi, Effects of ring substituents on the protective properties of self-assembled benzenethiols on copper, Corros. Sci. 48 (2006) 840–862.
[44] C. Li, L. Li, C. Wang, Y. Zhu, W. Zhang, Study of the protection performance of self-assembled monolayers on copper with the scanning electrochemical microscope, Corros. Sci. 80 (2014) 511–516.
[45] Z. Chen, L. Huang, G. Zhang, Y. Qiu, X. Guo, Benzotriazole as a volatile corrosion inhibitor during the early stage of copper corrosion under adsorbed thin electrolyte layers, Corros. Sci. 65 (2012) 214–222.
[46] P. Song, X.Y. Guo, Y.C. Pan, S. Shen, Y. Sun, Y. Wen, H.F. Yang, Insight in cysteamine adsorption behaviors on the copper surface by electrochemistry and Raman spectroscopy, Electrochim. Acta 89 (2013) 503–509.
[47] El-Sayed M. Sherif, R.M. Erasmus, J.D. Comins, Inhibition of copper corrosion in acidic chloride pickling solutions by 5-(3-aminophenyl)-tetrazole as a corrosion inhibitor, Corros. Sci. 50 (2008) 3439–3445.
[48] T.T. Qin, J. Li, H.Q. Luo, M. Li, N.B. Li, Corrosion inhibition of copper by 2,5-dimercapto-1,3,4-thiadiazole monolayer in acidic solution, Corros. Sci. 53 (2011) 1072–1078.
[49] E.M. Sherif, S.M. Park, Effects of 2-amino-5-ethylthio-1,3,4-thiadiazole on copper corrosion as a corrosion inhibitor in aerated acidic pickling solutions, Electrochim. Acta 51 (2006) 6556–6562.
[50] A. Lalitha, S. Ramesh, S. Rajeswari, Surface protection of copper in acid medium by azoles and surfactants, Electrochim. Acta 51 (2005) 47–55.
[51] X.R. Ye, X.Q. Xin, J.J. Zhu, Z.L. Xue, Coordination compound films of 1-phenyl-5-mercaptotetrazole on copper surface, Appl. Surf. Sci. 135 (1998) 307–317.
[52] M. Finsgar, I. Milosev, Inhibition of copper corrosion by 1,2,3-benzotriazole: a review, Corros. Sci. 52 (2010) 2737–2749.
[53] M. Finšgar, 2-Mercaptobenzimidazole as a copper corrosion inhibitor: Part II. Surface analysis using X-ray photoelectron spectroscopy, Corros. Sci. 72 (2013) 90–98.
[54] M. Finšgar, D.K. Merl, Mercaptobenzoxazole as a copper corrosion inhibitor in Chloride Solution: Electrochemistry, 3D-Profilometry, and XPS Surface Analysis, Corros. Sci. 80 (2014) 82–95.
[55] M. Finšgar, 2-Mercaptobenzimidazole as a copper corrosion inhibitor: Part I. Long-term immersion, 3D-profilometry, and electrochemistry, Corros. Sci. 72 (2013) 82–89.
[56] D. Zhang, L. Gao, G. Zhou, Inhibition of copper corrosion in aerated hydrochloric acid solution by heterocyclic compounds containing a mercapto group, Corros. Sci. 46 (2004) 3031–3040.
[57] J.P. Adams, Imines, enamines and oximes, J. Chem. Soc. Perkin Trans. 1 (2000) 125–139.
[58] J. Gawronski, N. Wascinska, J. Gajewy, Recent progress in Lewis base activation and control of stereoselectivity in the additions of trimethylsilyl nucleophiles, Chem. Rev. 108 (2008) 5227–5252.
[59] M. Pourbaix, Atlas of Electrochemical Equilibrias in Aqueous Solutions, National Association of Corrosion Engineers, Houston, TX, 1996.
[60] O.E. Barcia, O.R. Mattos, N. Pébère, B. Tribollet, Anodic dissolution of metals under mass transport control, Electrochim. Acta 41 (1996) 1385–1391.
[61] Q.A. Huang, R. Hui, B. Wang, J. Zhang, A review of AC impedance modeling and validation in SOFC diagnosis, Electrochim. Acta 52 (2007) 8144–8164.
[62] T. Tuken, F. Demir, N. Kicir, G. Sigircik, M. Erbil, Inhibition effect of 1-ethyl-3-methylimidazolium dicyanamide against steel corrosion, Corros. Sci. 59 (2012) 110–118.
[63] J. Bockris, A.K.N. Reddy, M. Gamboa-Aldeco, Modern Electrochemistry, vol. 2A, Kluwer Academic/Plenum Publishers, New York, 2000.